Concentration Enrichment in Confined, Gradient Energy Systems

Timothy J. Kosto II and E. Bruce Nauman
Howard P. Isermann Dept. of Chemical and Biological Engineering, Rensselaer Polytechnic Institute, Troy, NY 12180

DOI 10.1002/aic.10422
Published online in Wiley InterScience (www.interscience.wiley.com).

The enrichment or depletion of components near bounding surfaces in confined geometries was estimated using the generalized chemical potential for a molecule in a binary mixture. The chemical potential depends on concentration gradients and the local concentrations. Mean-field–based parameter estimates were combined with regular solution thermodynamics to calculate the enrichment of the favored component near an attractive bounding surface in confined geometries arising from weak van der Waals attractions. Partition coefficients from 2 to 3000 were calculated for pores of small but realistic diameter in contact with a reservoir of the binary mixture. Critical wetting transitions, like those reported for unconfined systems, occurred in confined pores. In such a transition, the material inside is near the upper binodal concentration when the reservoir concentration is below the lower binodal. The corresponding partition coefficient is then very large; appreciable concentration enrichment occurs even in pores that do not exhibit wetting transitions. © 2005 American Institute of Chemical Engineers
AIChE J, 51: 1032–1041, 2005

Introduction

Binary mixtures near interfaces may exhibit enrichment or depletion in a component as a result of interactions between the bounding surface and the mixture components (Jerry and Dutta, 1994). The magnitude of the enrichment is determined by the strength of the interaction between components and the wall and the energy required to form the necessary gradients in concentration. In immiscible systems, strong interactions between one component and the wall can cause the attracted phase to wet the wall (Binder et al., 2001; Cahn, 1977; Engels and Leermakers, 2001; Flebbe and Duenweg, 1996). Favorable interactions between the wetting phase and the bounding surface cause this wetting transition to occur.

Surface effects become particularly important in high surface area systems including dispersions, films, porous structures, and confined geometries. Changes in mixture concentrations near surfaces have been experimentally observed in many systems (Ebbens and Badyal, 2001; Guo et al., 2000; Hojun and Archer, 2002; Liu et al., 2000; Yuan and Shoichet, 2000). Particularly in confined regions, the proximity of interacting surfaces may lead to significant partition coefficients when the interaction distance exceeds the half-width of the pore. A classic example is the electric double layer in charged colloidal systems. Overlapping double layers raise the electric potential in the region between the two particles to greater than its value in the bulk solvent. Similar effects have been predicted around particles in systems in which only van der Waals interactions are present (Kinoshita, 2000). Narrow pores exhibit analogous behavior. Porous chromatographic gels that selectively attract a particular mixture component will enhance the efficiency of a separation by similar means, compared to size-exclusion chromatography in chemically neutral gels.

Nanometer-scale systems are increasingly common both in the academic literature and in industrial practice. The interactions on the nanometer scale may also be seen in some micron-scale systems, which are even more common, particularly in catalysis and separation systems. Nanometer-scale flow systems are used in lab-on-a-chip technologies for biological analysis and high-throughput screening for drug discovery. On these scales care must be taken to ensure that material is not constrained by interactions with the boundaries. In separation systems, interactions between the porous media and a component in the feed stream can be used to enhance the effectiveness of the separation so that the purity of the product can be increased, compared to a simple size-exclusion technique. In carbon nanotubes, numerous studies have been undertaken to

Correspondence concerning this article should be addressed to T. J. Kosto II at this current address: Taconic, PO Box 69, Petersburgh, NY 12138; e-mail: tjk095@alumni.lehigh.edu.

investigate the enrichment of particular materials inside the nanotube. In any of these techniques, several different interactions may contribute to the attraction or repulsion of a material from the surface. In this study, the influence of van der Waals interactions is evaluated in nanometer-scale pores.

Many examples of equilibrium studies in confined geometries exist in the literature, although most contemporary works report the results of atomistic simulations over small regions and timescales (Cifra and Teraoka, 2002; Svensson and Woodward, 1994). Alternatively, continuum mechanics provides a technique to study the time-average behavior of these systems, even on very small scales; they also require fewer computational resources in general. Continuum systems, including mean-field theories, capitalize on the time averages of localized disturbances on the small scale, effectively predicting observed physical behavior despite the lack of accurate dynamic representations of the nanoscale processes occurring in systems that are dynamically modeled using stochastic simulation techniques.

Background

The Cahn model

The total free energy of density- or concentration-variant systems is given by the Landau–Ginzburg functional

$$G = \int\int\int_V \left[g + \frac{\kappa}{2} (\nabla a)^2 \right] dV \tag{1}$$

Here a is the fluid concentration as a function of position, g is a homogeneous free energy of mixing, and κ is the gradient energy parameter. The Landau–Ginzburg functional requires the following two conditions (Debye, 1959)

$$\int_S (\nabla a \cdot n) ds = 0$$

$$\int_S [a(\nabla a \cdot n)] ds = 0 \tag{2}$$

where S is the bounding surface and n is the unit normal extending from the bounding surface. In general, these conditions are met only by periodic systems or systems with no concentration gradient at the boundaries (neutral walls) (Jerry and Nauman, 1992a). In nonperiodic systems with boundary gradients, the integrals of Eq. 2 are absorbed into a boundary penalty term, Φ, which is added to the Landau–Ginzburg functional

$$G = \Phi + \int\int\int_V \left[g + \frac{\kappa}{2} (\nabla a)^2 \right] dV \tag{3}$$

Cahn (1977) recognized that the boundary penalty term must depend on the limiting concentration of the fluid at the boundary, although he proposed no functional form for Φ.

The boundary penalty term

Several proposed forms for the surface energy exist in the literature. Some are based on phenomenological analyses, like that of Schmidt and Binder (1985) who assume the penalty term to be quadratic in the wall concentration. Cohen and Muthukumar (1989) developed an expression for the wall concentration based only on short-range interactions between the wall and the mixture. Jerry and Nauman (1992b) relaxed the short-range restriction, deriving expressions for the boundary term by extending the work of Debye. Both the Cohen–Muthukumar and Jerry–Nauman expressions permit functions of the wall concentration and its derivatives in the boundary penalty.

The physical basis of the boundary energy term is identical to that for surface tension. In a fluid exposed to vacuum, the normal bulk structure is perturbed at the surface where the last molecular layer has no interaction with molecules in the direction normal to the surface, extending into the vacuum. In a bounded fluid, the interaction between fluid molecules is replaced by an interaction with the molecules in the wall, which may be more or less favorable than interactions with itself as in a bulk fluid. Using mean-field theory, Jerry and Nauman derived the following expression for the boundary penalty in a fluid adjacent to a wall

$$\Phi = \frac{VC}{k_B T} \left[\xi'(a_{0^+}) - \frac{1}{2} \xi(a_{0^+}) \right] \tag{4}$$

The boundary penalty of Eq. 4 depends on the molar volume V; the number of contacts between a molecule and the wall C; the temperature; Boltzmann constant; and a function $\xi(a_{0^+})$, which depends on the interaction energies between the mixture components and the wall molecules. A simplified model is appropriate when the wall is composed of the same molecules as those in the mixture, albeit frozen (or crosslinked, in the case of a polymer) at some fixed composition. In this case, Eq. 4 has the following form (Jerry and Nauman 1992c)

$$\Phi = \frac{2\chi_{AB}}{Z} \left[\frac{1}{2} a_{0^+}^2 - a_{0^+} a_{wall} \right] + \frac{1}{k_B T} \left[\frac{a_{wall}}{2} \varepsilon_{AB} + \left(\frac{1}{2} - a_{wall} \right) \varepsilon_{BB} \right] \tag{5}$$

In this expression, χ_{AB} is the interaction parameter between the mixture components, Z is the coordination number of the lattice used in the mean field model, ε is the interaction energy between two molecules, and a_{wall} is the concentration of component A in the frozen wall. Equation 5 will be used in the development of a free energy expression for open pores.

Mathematical Development

The generalized chemical potential

This study is undertaken to investigate the influence of gradient energy effects in narrow pores with interacting walls. Like previous studies by Jerry and Nauman (1992a–c) in systems with interacting boundaries, the free energy in this system is based on a modified form of the Landau–Ginzburg functional:

$$G = \Phi + \int\int\int_V \left[g + \frac{\kappa}{2} (\nabla a)^2 \right] dV \tag{6}$$

Nauman and Balsara (1989) derived a generalized chemical potential from the variational free energy for systems without a boundary penalty term. The variational free energy Υ is defined by Eqs. 7 and 8

$$\left(\frac{\partial \Upsilon}{\partial a}\right)_b = \left(\frac{\delta G_{Total}}{\delta a}\right) = \left(\frac{\partial G}{\partial a}\right)_{b,\nabla a,\nabla b} - \nabla \cdot \left[\frac{\partial G}{\partial(\nabla a)}\right]_{a,b,\nabla b} \quad (7)$$

$$\left(\frac{\partial \Upsilon}{\partial b}\right)_a = \left(\frac{\partial G_{Total}}{\partial b}\right) = \left(\frac{\partial G}{\partial b}\right)_{a,\nabla a,\nabla b} - \nabla \cdot \left[\frac{\partial G}{\partial(\nabla b)}\right]_{a,b,\nabla a} \quad (8)$$

Integrating Eqs. 7 and 8 gives the variational free energy from which the chemical potentials are found using Eqs. 9 and 10, as derived by Nauman and Balsara (1989)

$$\mu_A = \Upsilon + b\left[\left(\frac{\partial \Upsilon}{\partial a}\right)_b - \left(\frac{\partial \Upsilon}{\partial b}\right)_a\right] \quad (9)$$

$$\mu_B = \Upsilon + a\left[\left(\frac{\partial \Upsilon}{\partial b}\right)_a - \left(\frac{\partial \Upsilon}{\partial a}\right)_b\right] \quad (10)$$

When the total free energy G_{total} is given by the modified Landau–Ginzburg functional of Eq. 6, the variational free energy is

$$\Upsilon = g - \frac{\kappa}{2}(\nabla a)^2 + C \quad (11)$$

Nauman and Balsara (1989) took the constant of integration in Eq. 11 to be zero. In the current system, the constant of integration is found using thermodynamic equilibrium requirements. The chemical potentials based on the variational free energy of Eq. 11 are

$$\mu_A = g - \frac{\kappa}{2}(\nabla a)^2 + (1 - a)(g' - \kappa\nabla^2 a) + C \quad (12)$$

$$\mu_B = g - \frac{\kappa}{2}(\nabla a)^2 + -a(g' - \kappa\nabla^2 a) + C \quad (13)$$

In transient systems, the chemical potential is a function of position. At equilibrium, the chemical potential must be constant everywhere. In an open system at equilibrium with its surroundings, the chemical potential everywhere inside the pore must be equal to that in the surroundings

$$\mu_A = \mu_{A,res} \quad (14)$$

The equality of Eq. 14 is applied at a point in the domain to determine the constant in Eqs. 12 and 13. The selection of an appropriate point to apply Eq. 14 is based on the domain geometry.

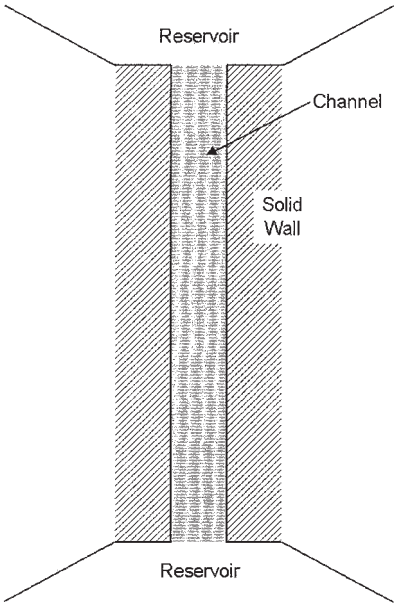

Figure 1. Narrow pore geometry.

Domain geometry

The system of interest is a long, narrow pore containing a binary fluid mixture, as shown in Figure 1. The pore is open at each end to an infinite reservoir containing the same binary mixture at a concentration such that it is everywhere homogeneous. The long boundaries are frozen walls at a fixed concentration, as shown in the figure. The mathematical formulation of this problem does not restrict the volume fractions in the wall to the range [0, 1]. The wall "concentration" is based on interaction energies between the two solution species and whatever species makes up the wall. All of the interactions are attractive, so a wall that is more like component A (that is, has a higher attractive potential to component A than to component B: $\varepsilon_{a,wall} > \varepsilon_{b,wall}$) will tend to attract component A. The situation of a wall "concentration" > 1 may occur when the wall has a greater density than the fluid or when the fluid is an amphiphile, whereas the wall corresponds to only one of the two ends of the amphiphilic molecule. A neutral wall has a concentration equal to the concentration of the fluid in the reservoir, has no selective attractive potential with either component, and would produce a uniform concentration everywhere inside the pore. The actual value of the frozen wall concentration conceptually represents the strength of attraction between the wall and the species in solution rather than a real physical concentration. However, walls of varying concentration can be physically achieved, such as by forming the wall from polymerized or crosslinked versions of the components in the fluid phase.

The homogeneous free energy of the fluid is given by regular solution theory and is scaled by thermal energy

$$g = a\ln(a) + b\ln(b) + \chi ab \quad (15)$$

Distances are scaled by the molecular size.

When the pore aspect ratio is very large, end effects may be neglected, eliminating axial dependency in the problem. No

driving forces exist to cause gradients in the angular directions so the problem becomes one-dimensional in the radial direction. The solution must also be symmetric with respect to the centerline, where the derivative in concentration must be zero. The equivalence of chemical potentials in Eq. 14 is applied at the centerline to determine the value of the constant in Eq. 11. The difference between Eqs. 12 and 13 gives Eq. 16, which can be used to simplify Eq. 12

$$g' - \kappa\nabla^2 a = \mu_A - \mu_B \tag{16}$$

Substituting the simplified form of Eq. 12 into the equality of Eq. 14 gives an expression for the integration constant in Eq. 11

$$\begin{aligned} C &= \mu_A - g_{CL} - (1-a)(\mu_A - \mu_B) \\ &= \mu_A - g_{CL} - (1-a)\, g'_{res} \end{aligned} \tag{17}$$

Equation 12 can now be rearranged, yielding a first-order, ordinary differential equation for the concentration in the radial direction

$$\frac{da}{dr} = \left\{ \frac{2}{\kappa} \left[g - g_{CL} + (a_{CL} - a)\, g'_{res} \right] \right\}^{1/2} \tag{18}$$

The appropriate boundary conditions are found by using the variational calculus, including the boundary penalty term in Eq. 6. Using Eq. 5 for the functional dependency of the boundary penalty, the boundary conditions at the wall and the centerline become

$$\begin{aligned} \left.\frac{da}{dr}\right|_{wall} &= \frac{2\chi}{Z\kappa}\,(a_{wall^-} - a_{wall}) \\ \left.\frac{da}{dr}\right|_{CL} &= 0 \end{aligned} \tag{19}$$

Equation 18 may be integrated, subject to the boundary conditions of Eq. 19, to give the concentration profile in the pore.

Parameter definitions

For any given parameter set, integrating and normalizing the concentration profile yields the average concentration in the pore. The ratio of this average concentration to the reservoir concentration defines the partition coefficient

$$K = \frac{\bar{a}}{a_{res}} \tag{20}$$

A second parameter quantifies the effectiveness of the wall. The wall efficiency η_{wall} characterizes how strong an influence the wall exerts compared to that of the reservoir. The reservoir influence is dominant in a wide pore, yielding low wall efficiencies. In narrow pores, the walls dominate, resulting in high wall efficiencies. The wall efficiency is defined as

$$\eta_{wall} = \frac{\bar{a} - a_{res}}{a_{wall} - a_{res}} \tag{21}$$

This parameter represents the total enrichment as a fraction of the difference between the reservoir and the wall concentrations.

Numerical Studies

Solution multiplicity

Several techniques are appropriate to find the equilibrium concentration in a narrow pore. The first-order ordinary differential equation (ODE) in Eq. 18 may be integrated from the center to the wall or in the reverse direction. This technique works well for pores of small diameter, but requires unfeasibly high precision for large pores and for certain other parameter values. Typically, the equations are solved by guessing either a near wall concentration or a centerline concentration and then integrating to the opposing boundary. For the ill-conditioned case of large diameter pores, changing the guess by one unit in the sixteenth decimal place may give a negative concentration at some point during the integration, whereas a change of one unit in the opposite direction results in a positive derivative at the centerline (which does not fulfill the boundary condition at the centerline), or in some cases a domain concentration that exceeds unity, which—inside the pore—is not feasible. The ill-conditioning is exacerbated as the pore diameter increases; it is similarly aggravated by high interaction parameters and low reservoir concentrations.

Integration of the Euler equation, found using the variational calculus, increases the numerically feasible region

$$\frac{dg}{da} - \left.\frac{dg}{da}\right|_{a_{res}} - \kappa\nabla^2 a = 0 \tag{22}$$

All these techniques require the boundary conditions of Eq. 19 and generate identical concentration profiles in the pore. There are numerically feasible regions where all four solution techniques produce multiple mathematically valid solutions. In cases where multiple solutions occur, the global minimum is identified by calculating the total free energy difference between each solution and a reference state having neutral walls and a uniform composition in the pore

$$\Delta G = \Phi + \int_0^R \left[g - g_{res} + \frac{\kappa}{2} \left(\frac{da}{dr} \right)^2 \right] dr \tag{23}$$

The concentration profile corresponding to the global minimum is integrated to facilitate calculating the average concentration in the pore at equilibrium. Figure 2 shows the average concentration in the pore (solid line) as a function of the pore radius when the wall is composed of pure A. The grayed region of the figure identifies the zone of multiple solutions. Very narrow and wide pores have single, unique solutions. Because the average concentration in the pore should vary inversely with increasing pore radius, the region of positive slope (fine solid line) is disregarded as nonphysical. Equation 23 is evaluated for each of the two remaining solutions and plotted as a dotted line in the figure. The upper free energy profile corresponds to the lower average concentration and the lower free energy line corresponds to the upper average concentration profile. The global minimum occurs at the integrated concentration profile giving the higher average concentration in the

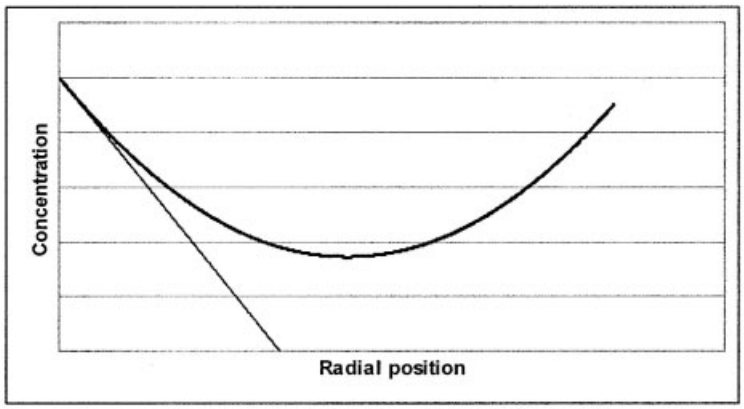

(a)

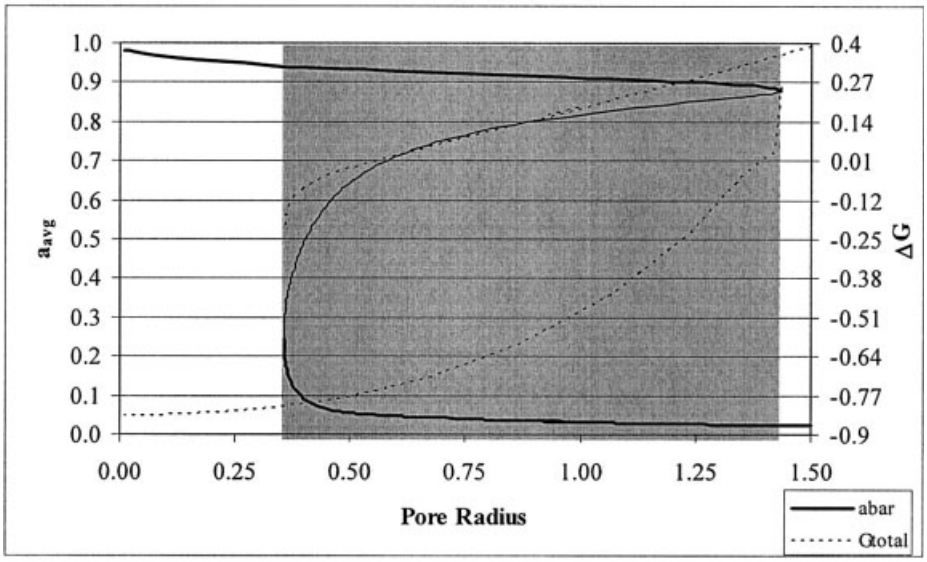

(b)

Figure 2. (a) Concentration as a function of radial position; (b) average concentration and ΔG profiles as a function of the pore radius.

The plot in (a) shows an example of the ill-conditioning observed in the solutions to the differential equations. The difference in the guess of the near wall concentration for this set of conditions is at the limit of numerical precision. The actual concentration profile lies somewhere in the intermediate region, although its exact position cannot be known based on these two profiles that bracket the correct solution. The gray region in (b) identifies the multiple solution zone. The fine solid line indicates a mathematically valid, nonphysical result.

pore. A wetting transition occurs at $r_{pore} = 1.43$. At that point, the free energy profile of the upper average concentration increases rapidly toward an intersection with the free energy profile from the lower average concentration line. For $r_{pore} > 1.43$ the lower profile indicates the correct and unique solution. Wetting transitions are also observed with increasing wall concentration, increasing interaction parameter, and increasing reservoir concentration. In the first two cases, the driving force for enrichment is stronger. In the last case, the barrier to wetting is reduced by raising the reservoir concentration. Parameter studies were undertaken to look for similar transitions and evaluate the concentration enrichment.

Influence of the wall concentration

Parameter studies investigated the influence of the wall composition on the average pore concentration and the partition coefficient. Figure 3 shows the results. Higher wall concentrations provide greater driving force to draw material from the reservoir into the channel. As a result, the average concentration in the channel increases with increasing wall concentration. At some wall concentration, the required gradient in concentration across the pore becomes too steep and the enriched material wets the wall, essentially filling the pore. This wetting transition occurs at $a_{wall} = 0.99$ when $\chi = 5$. When $\chi = 3$, there is insufficient driving force to cause wetting, although a wetting transition would presumably occur at much higher wall concentrations. The average concentration increases, albeit without a wetting transition in the region studied. Figure 4 shows the wall efficiency for these studies. Up to the wetting transition, the wall efficiency increases with the wall concentration. However, after the wetting transition, the wall efficiency decreases with increasing wall concentration as a consequence of the physical limitation to a maximum mass frac-

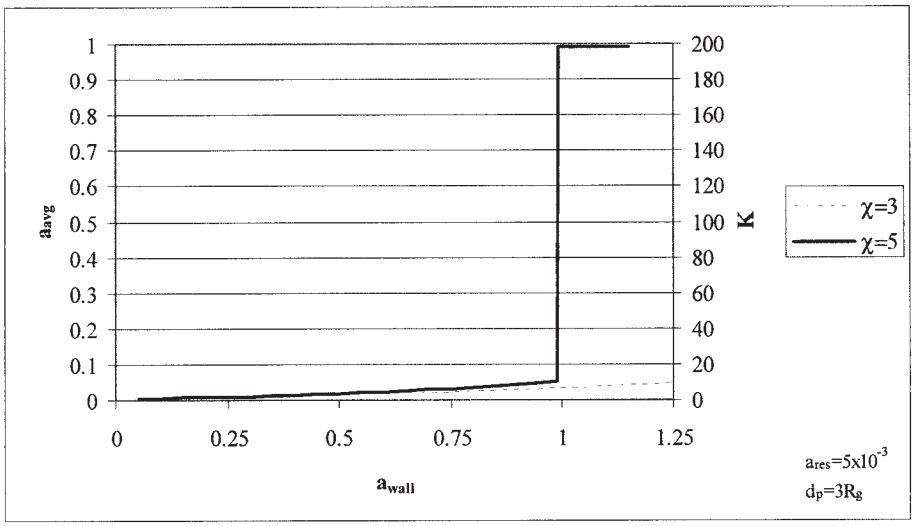

Figure 3. Average concentration and partition coefficient profiles as a function of the wall composition.

Wall compositions exceeding unity represent a wall composed of a material that has a stronger interaction with component A than component A has with itself.

tion of unity. As the wall concentration approaches infinity, the wall efficiency must vanish

$$\lim_{a_{wall}\to\infty} (\eta_{wall}) = 0 \tag{24}$$

Therefore, in a wetting system, the maximum wall efficiency will occur at or slightly above the wetting point. For a nonwetting system, the wall becomes more efficient as its effective concentration increases. From a separations design perspective, the appropriate design characteristic is a maximum concentration not to exceed the composition required to achieve wetting. The results from this set of comparisons indicate that higher interaction parameters (less miscible components) enhance the enrichment.

The interaction parameter effect

Using a reservoir concentration $a_{res} = 2 \times 10^{-3}$, the influence of the interaction parameter was investigated. Figure 5 shows profiles at two wall concentrations, $a_{wall} = 0.5$ and $a_{wall} = 1.0$. In each case, the average pore concentration increases with increasing interaction parameter. Higher interaction parameters indicate less miscible mixture components resulting in stronger segregation. As a result, the wall will increasingly prefer like molecules from the mixture in its vicinity, raising the concentration profile and, consequently, the average concentration in the pore. When the mixture components are very immiscible (high interaction parameter), a wetting transition will occur. In the higher wall concentration case, such a wetting

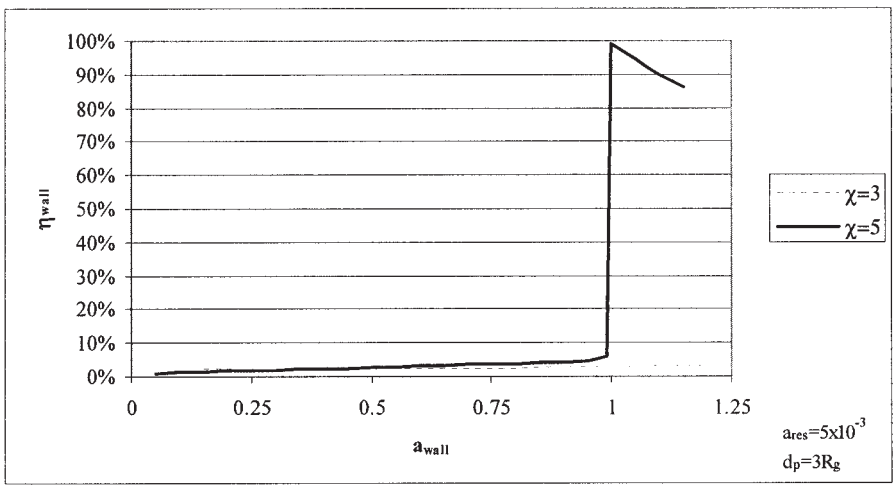

Figure 4. Wall efficiency profiles as a function of the wall composition.

Wall compositions exceeding unity represent a wall composed of a material that has a stronger interaction with component A than component A has with itself.

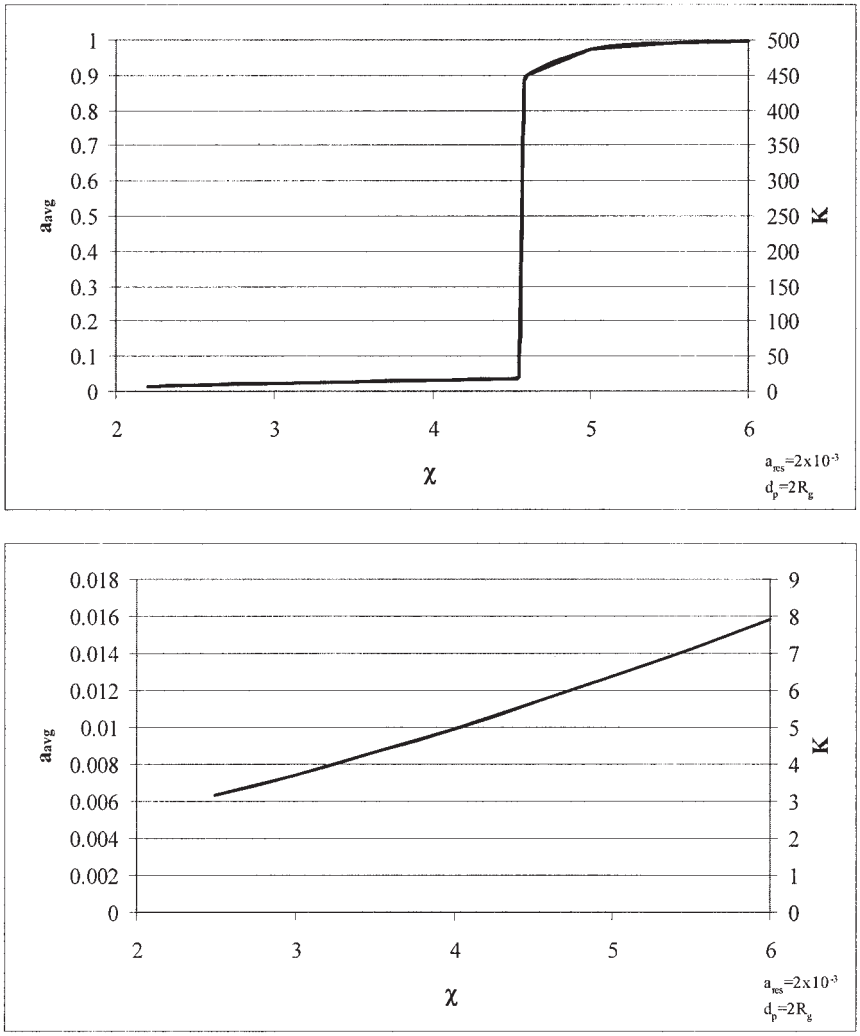

Figure 5. (a) Average concentration and partition coefficient profiles as a function of the interaction parameter for the case a_{wall} = 1.0; (b) average concentration and partition coefficient profiles as a function of the interaction parameter for the case a_{wall} = 0.5.

transition occurs at $\chi = 4.55$. Although wall concentrations less than the upper binodal are capable of inducing a wetting transition, such a situation would require a very high interaction parameter, which makes the problem numerically infeasible. As a result, only high wall concentrations exhibit wetting transitions in this study.

Reservoir concentration effects

Because of numerical ill-conditioning of the differential equation, a relatively small range of reservoir concentrations are computationally feasible at a fixed interaction parameter. Figure 6 shows the results for $\chi = 5.5 \times 10^{-4} \leq a_{res} \leq 7 \times 10^{-3}$. A wetting transition is observed in this case at $a_{res} = 9 \times 10^{-4}$. Although the average concentration profile is consistent with physical intuition, Figure 7 shows an intriguing result regarding the partition coefficient. Disregarding the wetting transition, the partition coefficient increases as the reservoir concentration decreases. This result suggests that a enrichment becomes more effective as the concentration of solute in the bulk phase decreases. Although numerical results for very low reservoir concentration are infeasible, the results that were obtained indicate that the optimal enrichment occurs at the wetting transition, consistent with studies of the variable wall concentration shown in Figure 4.

Solutions for large-diameter pores

All the results reported above apply to pores less than three molecular diameters across. Clearly, larger pores are more interesting, but small-diameter pores alleviate the numerical sensitivity, allowing study of broader parameter ranges. However, some assessment of the enrichment in a larger pore is possible. Figure 8 shows the effect of the pore diameter for two cases. The average pore concentration decreases with increasing pore diameter, although the slope is quite small in magnitude. The wetting transitions occur at moderate widths, $d_{pore} = 4.0$ when $\chi = 5$ and $d_{pore} = 12.2$ when $\chi = 3$. In both cases, the pore is wet by a fluid phase (binodal composition), not by a component. The wetting-phase composition is a function of the solution-phase diagram. At 12 molecular diameters, molecules should be able to enter and vacate the pore with relative

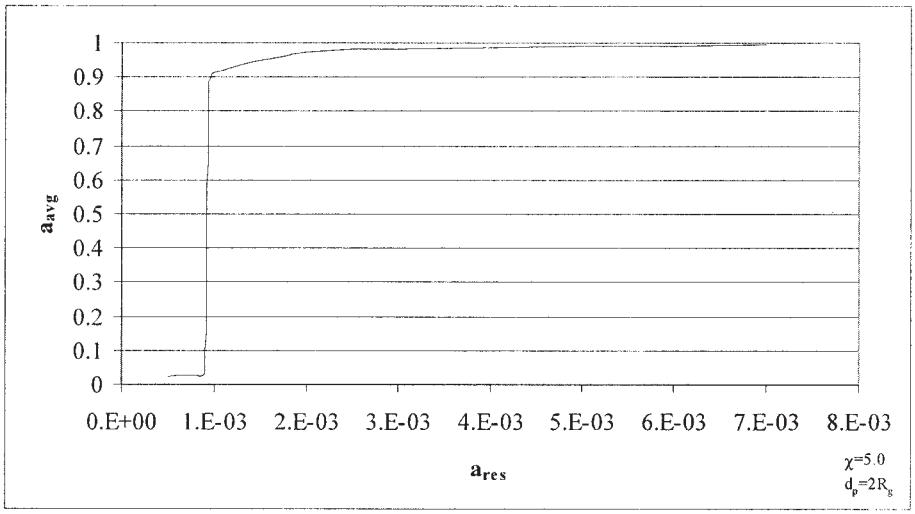

Figure 6. Average concentration profile as a function of the reservoir concentration.

ease. However, even in large pores that do not wet, average concentrations in the pore can be several orders of magnitude higher than reservoir concentrations, especially as the interaction parameter increases.

Increases in partition coefficient are observed with both increasing interaction parameter and decreasing reservoir concentration (Figures 5 and 7). The combined effect of low reservoir concentrations and high interaction parameter was studied for $10 \leq \chi \leq 25$. Table 1 shows the wall concentrations and consequent partition coefficients for several cases where $d_{pore} = 1$. Remarkably, the partition coefficient increases from only 10^3 at $\chi = 10$ to $>10^9$ at $\chi = 25$. Interaction parameters $>$ 25 are realistic for polymer systems; they yield even higher partition coefficients. These high partition coefficients show that gradient energy effects are quite powerful at very low solute concentrations in the bulk phase.

This final observation suggests that nanoscale pores used as separating devices would operate most effectively at very low solute concentrations. Certainly, a process stream should not be diluted for separating based on improved relative efficiency. Rather, a separation system found to operate in this fashion should be used where low solute concentrations are the specified feedstock. Such a condition could well occur in natural systems such as environmental pollutants in waterways where the actual concentrations are at the level of billionths and trillionths. Another naturally occurring condition that may be encountered is the presence of minute amounts of blood toxins that have resulted from industrial and general exposure to synthetic chemicals.

Conclusions

The classical thermodynamic condition of equilibrium—equality of chemical potential—has been used to determine concentration profiles in narrow, high aspect ratio channels. The mathematical formulation is based on the Landau–Ginzburg functional, which is extended to open pores. Parameter estimates were obtained from mean-field theories and are appropriate to weak van der Waals attractions between the components of a binary mixture. The resulting differential equations were numerically integrated. The results are consistent with physical intuition and they show increased enrichment for narrower pores, higher wall interactions with the minor component, and

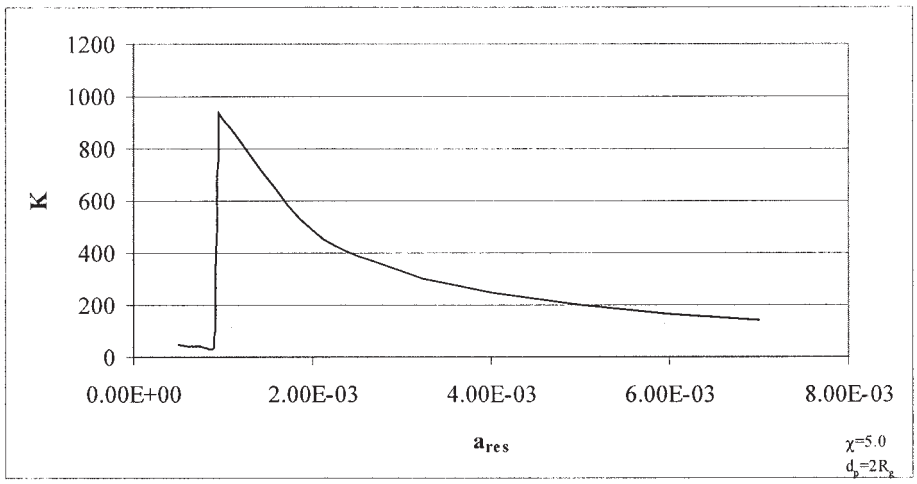

Figure 7. Partition coefficient as a function of the reservoir concentration.

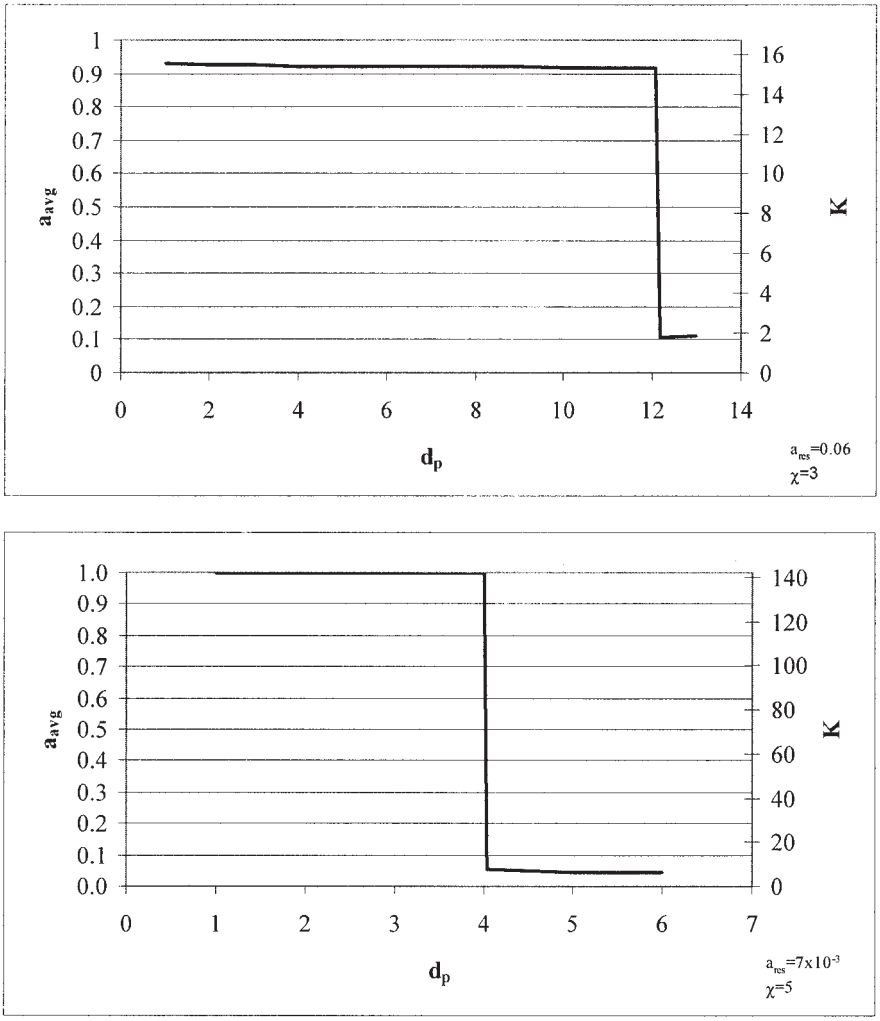

Figure 8. (a) Average concentration profile as a function of pore diameter (the wetting transition occurs at d_p = 12.2); (b) average concentration profile as a function of pore diameter (the wetting transition occurs at d_p = 4.0).

increasing interaction parameter between the components. With small pores and high reservoir concentrations, a critical wetting transition was observed in which the cross section of the pore is at the upper binodal concentration. Lower reservoir concentrations and larger pores do not exhibit critical wetting but can still show significant enrichment of the minor component when it is selectively attracted to the pore walls. Although not included in the present studies, some enrichment can be expected even for compatible mixtures with $\chi < 2$. For a fixed χ and pore diameter, the partition coefficient increases with lower reservoir concentrations; the pore becomes more effective at drawing material into itself as the reservoir concentration is decreased.

Table 1. Data for Several High χ Values

χ	a_{wall}	a_{avg}	K	η_{wall}
10	1.00	0.069	1.54E+03	6.94%
15	1.00	0.048	1.58E+05	4.78%
20	1.25	0.088	4.30E+07	7.02%
25	1.25	0.069	5.02E+09	5.52%

The partition coefficient increases with decreasing reservoir concentration (and increasing χ). The average concentration decreases with increasing χ value, at each wall composition.

These equilibrium studies provide a starting point in the design of separation systems, but an estimate of the dynamics is also required. The estimate could use the continuum mechanical, mean-field approach of the present paper (such as the diffusion equation), but for very small pores, molecular dynamics could be used to estimate the time needed to approach equilibrium.

Notation

a = concentration fraction of component A
b = concentration fraction of component B
C = interaction points between a solution molecule and the domain wall
g = homogeneous free energy
G = total free energy
K_B = Boltzmann constant
n = unit normal to a surface
R = pore radius
S = surface
T = temperature, K
V = volume
x, y, r = spatial coordinates in Cartesian and cylindrical coordinate systems, respectively
Z = lattice coordination number

Greek letters

Φ = boundary contribution to the total free energy
Υ = variational free energy
χ = Flory–Huggins interaction parameter
ε = binary interaction energy
κ = gradient energy parameter
μ = chemical potential
η = enrichment efficiency

Literature Cited

Binder, K., M. Muller, and E. V. Albano, "Symmetric Binary Polymer Blends Confined in Thin Films between Competing Walls: Interplay between Finite Size and Wetting Behavior," *Phys. Chem. Chem. Phys.*, **3**, 1160 (2001).

Cahn, J. W., "Critical Point Wetting," *J. Chem. Phys.*, **66**(8), 3667 (1977).

Cifra, P., and I. Teraoka, "Partitioning of Polymer Chains in Solution with a Square Channel: Lattice Monte Carlo Simulations," *Polymer*, **43**, 2409 (2002).

Cohen, S. M., and M. Muthukumar, "Critical Wetting in Two-Component Polymer Blends," *J. Chem. Phys.* **90**, 5749 (1989).

Debye, P., "Angular Dissymmetry of the Critical Opalescence in Liquid Mixtures," *J. Chem. Phys.*, **31**(3), 680 (1959).

Ebbens, S. J., and J. P. Badyal, "Surface Enrichment of Fluorochemical-Doped Polypropylene Films," *Langmuir*, **17**(13), 4050 (2001).

Engels, S. M., and F. A. M. Leermakers, "Wetting Transitions in Symmetrical Polymer Blends," *J. Chem. Phys.*, **114**(9), 4267 (2001).

Flebbe, T., B. Duenweg, et al., "Phase Separation versus Wetting: A Mean Field Theory for Symmetrical Polymer Mixtures Confined between Selectively Attractive Walls," *J. Phys. II*, **6**(5), 667 (1996).

Guo, S., L. Shen, et al., "Surface Characterization of Blood Compatible Amphiphilic Graft Copolymers Having Uniform Poly(ethylene oxide) Side Chains," *Polymer*, **42**(3), 1017 (2000).

Hojun, L., and L. Archer, "Funtionalizing Polymer Surfaces by Surface Migration of Copolymer Additives: Role of Additive Molecular Weight," *Polymer*, **43**(9), 2721 (2002).

Jerry, R. A., and A. Dutta, "The Enrichment-Depletion Duality as an Indicator of Critical Wetting in Polymer Blends," *J. Colloid Interface Sci.*, **167**, 287 (1994).

Jerry, R. A., and E. B. Nauman, "The Free Energy of a Binary Mixture Near a Surface with Applications to Surface Enrichment," *J. Colloid Interface Sci.*, **154**(1), 122 (1992a).

Jerry, R. A., and E. B. Nauman, "More Insight into Critical Wetting in Polymer Blends," *J. Chem. Phys.*, **97**(10), 7829 (1992b).

Jerry, R. A., and E. B. Nauman, "Phase Transitions in Thin Films of a Binary Mixture," *Phys. Lett. A*, **167**, 198 (1992c).

Kinoshita, M., "Binary Fluid Mixture Confined between Macroparticles: Surface-Induced Phase Transition and Long-Range Surface Forces," *Chem. Phys. Lett.*, **325**, 281 (2000).

Liu, B., H. Zhang, et al., "Surface Enrichment Effect on the Morphological Transitions Induced by Directional Quenching for Binary Mixtures," *J. Chem. Phys.*, **113**(2), 719 (2000).

Nauman, E. B., and N. P. Balsara, "Phase Equilibria and the Landau–Ginzburg Functional," *Fluid Phase Equilib.*, **45**, 229 (1989).

Schmidt, J., and K. Binder, "Model Calculations for Wetting Transitions in Polymer Systems," *J. Phys.*, **46**, 1631 (1985).

Svensson, B., and C. E. Woodward, "Simulations in Planar Slits at Constant Chemical Potential," *J. Chem. Phys.*, **100**(6), 4575 (1994).

Yuan, Y., and M. S. Shoichet, "Surface Enrichment of Poly(trifluorovinyl ether)s in Polystyrene Blends," *Macromolecules*, **33**(13), 4926 (2000).

Appendix

Although the equations used to investigate concentration enrichment in narrow pores were developed using thermodynamic arguments, the variational calculus may also be used to derive an appropriate Euler equation that will produce identical results based on the minimization of the total free energy in the system. As before, the total free energy in the pore is given by the modified Landau–Ginzburg functional of Eq. 3

$$G = \Phi + \int\int\int_V \left[g + \frac{\kappa}{2} (\nabla a)^2 \right] dV$$

Because the variational approach to this problem minimizes the total free energy, the free energy of the reservoir must also be included. The reservoir is infinite and its concentration does not change. Each unit of mass that crosses the boundary between the reservoir and the pore carries some energy with it. The total energy transferred is equal to the product of the partial molar energy multiplied by the total mass transferred. In constant temperature and pressure systems, the Gibbs free energy is used and the appropriate partial molar property is the chemical potential. Therefore, another term must be added to the functional

$$G = \Phi + \int\int\int_V \left[g + \frac{\kappa}{2} (\nabla a)^2 \right] dV + \int\int\int_V \mu_A(a_{res} - a) + \mu_B(b_{res} - b) dV$$

Recognizing that $a + b = 1$ and that the limits of integration are identical for both integral terms, the functional can be simplified

$$G = \Phi + \int\int\int_V \left[g + \frac{\kappa}{2} (\nabla a)^2 + g'_{res}(a_{res} - a) \right] dV$$

The variational derivative of this functional yields the following Euler equation

$$\frac{dg}{da} - \left. \frac{dg}{da} \right|_{a_{res}} - \kappa \nabla^2 a = 0$$

Additionally, the calculus of variations generates boundary conditions at the walls

$$\frac{\partial \Phi}{\partial a_{bound}} - \kappa \nabla a = 0$$

Rearranging the Euler equation gives a second-order partial or ordinary differential equation (depending on the dimensionality of the geometry under study), which can be integrated once analytically and once numerically, or twice numerically, to yield the concentration profile in the pore

$$\nabla^2 a = \frac{\dfrac{dg}{da} - \left. \dfrac{dg}{da} \right|_{a_{res}}}{\kappa}$$

The solutions to this differential equation are also solutions to Eq. 18 and therefore yield the same results as those presented above.

Manuscript received Jan. 6, 2003, revision received Apr. 6, 2003, and final revision received Nov. 22, 2004.